

SIMULATION OF WIDEBAND MOBILE RADIO CHANNELS USING SUBSAMPLED ARMA MODELS AND MULTISTAGE INTERPOLATION*

Dieter Schafhuber, Gerald Matz, and Franz Hlawatsch

Institute of Communications and Radio-Frequency Engineering, Vienna University of Technology
Gusshausstrasse 25/389, A-1040 Vienna, Austria
Tel.: +43 1 58801 38973, Fax: +43 1 58801 38999, E-mail: dschafhu@aurora.nt.tuwien.ac.at
web: <http://www.nt.tuwien.ac.at/dspgroup/time.html>

ABSTRACT

We present a technique for simulating time-varying mobile radio channels. This technique is specifically suited to the small relative Doppler bandwidths of wideband channels encountered in CDMA and OFDM communications. A “subsampled” ARMA innovations filter and multistage interpolation are used to achieve an accurate and computationally efficient approximation of specified or measured Doppler spectra (scattering functions). We discuss the calculation of the ARMA coefficients and the optimal design of the multistage interpolator. Simulation results demonstrate the excellent performance of the proposed channel simulator.

1. INTRODUCTION

Computer simulation of mobile radio channels is of great importance for the development and evaluation of mobile communications systems. A discrete-time channel model that is convenient for channel simulation is the time-varying tapped delay line (FIR filter) with input-output relation [1, 2]

$$y[n] = \sum_{m=0}^{M-1} h_m[n] x[n-m].$$

Here, $x[n]$ is the channel input signal, $y[n]$ is the channel output signal, $h_m[n]$ is the channel’s time-varying impulse response (with m the delay index and n the time index), and $M-1$ is the maximum delay. For *wide-sense stationary uncorrelated scattering* (WSSUS) channels, each tap weight sequence $h_m[n]$ is a stationary random process with autocorrelation function $r_m[l] = E\{h_m[n+l]h_m^*[n]\}$, and different tap weight processes $h_m[n]$, $h_{m'}[n]$ are uncorrelated [1, 2]. The power spectra of the $h_m[n]$,

$$S_m(\nu) = \sum_{l=-\infty}^{\infty} r_m[l] e^{-j2\pi\nu l}, \quad m = 0, 1, \dots, M-1,$$

are termed the channel’s *Doppler spectra* or *scattering function* [1, 2]. Here, ν is the Doppler frequency normalized by the sampling frequency. For wideband CDMA and OFDM systems, the sampling frequency is significantly higher than the channel’s maximum Doppler shifts. This results in extremely small Doppler bandwidths, i.e., the Doppler spectra $S_m(\nu)$ have extremely narrowband lowpass characteristics.

From the discussion above, it follows that the simulation of a WSSUS channel amounts to generating realizations of M uncorrelated, stationary tap processes $h_m[n]$ ($m =$

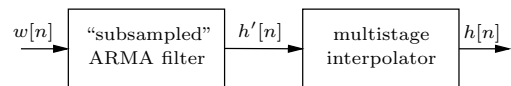


Figure 1: Structure of the proposed channel simulator: Generating a realization of a tap weight process $h_m[n]$.

$0, 1, \dots, M-1$) whose second-order statistics should conform to the specified $r_m[l]$ or, equivalently, $S_m(\nu)$. In this paper, we consider a tap process generator based on an *autoregressive moving-average* (ARMA) innovations filter [3, 4] that is driven by stationary white Gaussian noise. To avoid the high ARMA model order that would normally be needed for achieving the small relative Doppler bandwidths encountered in wideband CDMA and OFDM systems, we propose a “subsampled” ARMA innovations filter that is designed using a subsampled autocorrelation

$$r'_m[n] \triangleq r_m[nL]. \quad (1)$$

To compensate for the subsampling, the ARMA filter is followed by a *multistage interpolator* [5] for which we propose an MSE-optimal design. A block diagram of the resulting tap process generator is shown in Fig. 1. The generic structure of a channel simulator consisting of innovations filters and interpolators was previously considered in [6].

The proposed channel simulator has numerous advantages over other channel simulation techniques [1, 7–10]: the ARMA modeling approach allows accurate approximation of arbitrary Doppler spectra; arbitrarily long tap sequences can be generated online; new realizations are generated in each simulation run; the simulated channel is guaranteed to be Rayleigh fading; and finally, the multistage interpolator allows for efficient implementation, simplified interpolator filter design, and easy adjustment of the Doppler bandwidth without modification of the ARMA filter.

The rest of the paper is organized as follows. Section 2 discusses the subsampled ARMA innovations filter and presents methods for calculating the filter coefficients. Section 3 considers the multistage interpolator and its optimal design. Finally, simulation results are provided in Section 4.

2. ARMA INNOVATIONS FILTER

The subsampled ARMA innovations filter is an IIR filter described by the difference equation [3]

$$\sum_{k=0}^P a[k] h'[n-k] = \sum_{k=0}^Q b[k] w[n-k], \quad \text{with } a[0] \triangleq 1, \quad (2)$$

*This work was supported by FWF grant P11904-TEC.

where $a[k]$ and $b[k]$ are the autoregressive (AR) and moving-average (MA) coefficients, respectively, P and Q are the AR and MA model orders, respectively, $h'[n]$ is the filter output (the subsampled tap process; note that we suppress the subscript m in $h'_m[n]$ etc.), and $w[n]$ is the filter input that is chosen as white Gaussian noise. Multiplying (2) by $h'^*[n-l]$ and taking expectations yields [3]

$$\sum_{k=0}^P a[k] r'[l-k] = \sum_{k=0}^Q b[k] c^*[k-l], \quad l \in \mathbb{Z}, \quad (3)$$

where $r'[n] = r[nL]$ is the subsampled autocorrelation and $c[n]$ is the impulse response of the ARMA filter. This is a nonlinear equation in the ARMA coefficients $a[k]$ and $b[k]$ since $c[n]$ depends on $a[k]$ and $b[k]$.

In the frequency domain, (3) becomes

$$S'(\nu) = \frac{B(\nu)}{A(\nu)} C^*(\nu) = \frac{|B(\nu)|^2}{|A(\nu)|^2}, \quad (4)$$

where $S'(\nu)$, $A(\nu)$, $B(\nu)$, and $C(\nu) = B(\nu)/A(\nu)$ are the Fourier transforms of $r'[n]$, $a[n]$, $b[n]$, and $c[n]$, respectively.

For calculation of the AR and MA coefficients, the *specified* (subsampled) autocorrelation and Doppler spectrum are substituted for $r'[n]$ in (3) and for $S'(\nu)$ in (4), respectively. Typically, the ARMA model will only provide an approximation to the specified $r'[n]$ and $S'(\nu)$, and thus (3) and (4) will be satisfied only approximately.

2.1. Calculation of the AR Coefficients

Usually, the AR coefficients $a[n]$ are estimated from higher-lag (and, thus, smaller) values of $r'[n]$ that are not influenced by the MA model part [3]. However, here we include the central (largest) values of $r'[n]$ since we observed this to yield better accuracy of the overall ARMA approximation. This approach means that we first fit an AR filter and then fit an MA filter to the resulting residual autocorrelation. Formally setting $Q = 0$ and noting that the ARMA filter impulse response $c[n]$ is causal, (3) for $l = 1, 2, \dots, N$ together with $a[0] = 1$ yields the Yule-Walker equation [3]

$$\mathbf{R} \mathbf{a} = -\mathbf{r}, \quad (5)$$

where

$$\mathbf{R} = \begin{bmatrix} r'[0] & r'[-1] & \dots & r'[-P+1] \\ r'[1] & r'[0] & \dots & r'[-P+2] \\ \vdots & \vdots & \ddots & \vdots \\ r'[N-1] & r'[N-2] & \dots & r'[N-P] \end{bmatrix},$$

$\mathbf{a} = [a[1] \dots a[P]]^T$, and $\mathbf{r} = [r'[1] \dots r'[N]]^T$, with N the number of samples of $r'[n]$ that are used for the calculation. Equation (5) is a system of N linear equations in the P unknowns $a[n]$. For $N \geq P$, the least-squares solution of (5) (stabilized by diagonal loading [11, Chap. 7.4]) is given by

$$\mathbf{a} = -(\tilde{\mathbf{R}}^H \tilde{\mathbf{R}})^{-1} \tilde{\mathbf{R}}^H \mathbf{r}, \quad \text{with } \tilde{\mathbf{R}} = \mathbf{R} + \gamma \mathbf{I}.$$

Here, γ is a suitable loading parameter ensuring that all poles of the AR filter are inside the unit circle. For good results, N must be chosen much larger than P .

Criteria for selecting the AR model order P are discussed in [3]. However, it is also noted in [3] that these criteria seem to work well only for a true AR process. For a Doppler bandwidth of 10^{-4} and subsampling factor $L = 1000$, we obtained good results with $P = 10 \dots 50$ and $N = 3P \dots 10P$.

2.2. Calculation of the MA Coefficients

Once the AR coefficients $a[n]$ have been determined, we can proceed to calculate the MA coefficients $b[n]$. With *Durbin's method* [3,4], the MA modeling problem is transformed into two AR modeling problems of which one has significantly higher order than the MA model order Q . However, since in our case $Q = 100 \dots 1000$ to ensure good approximation accuracy, Durbin's method would be extremely expensive. Therefore, here we propose a modified version of the extended Prony method described in [3]. Our method is also related to the Blackman-Tukey spectral estimator [4].

Equation (4) can be rewritten as

$$|B(\nu)|^2 = |A(\nu)|^2 S'(\nu). \quad (6)$$

Basically, $b[n]$ can be obtained by causal factorization of $|B(\nu)|^2$. In the time domain, (6) reads

$$\beta[n] = \alpha[n] * r'[n], \quad (7)$$

with $\alpha[n] = a[n] * a^*[-n]$ and $\beta[n] = b[n] * b^*[-n]$. But from $\beta[n] = b[n] * b^*[-n]$, it follows that $\beta[n]$ should have finite support $[-Q, Q]$ and a nonnegative real Fourier transform. Therefore, we "correct" (7) by applying a Bartlett window to the right-hand side,

$$\beta[n] = \begin{cases} (\alpha[n] * r'[n]) \left(1 - \frac{|n|}{Q+1}\right), & |n| \leq Q \\ 0, & |n| > Q. \end{cases} \quad (8)$$

This enforces both finite support $[-Q, Q]$ and a nonnegative real Fourier transform (since the Fourier transforms of both $\alpha[n] * r'[n]$ and $1 - \frac{|n|}{Q+1}$ are nonnegative real). Finally, $b[n]$ is obtained by causal factorization of $\beta[n]$ [12, App. A]. To this end, the cepstrum of $\beta[n]$ in (8) is calculated [13]. Transforming the cepstrum's causal part back into the original domain yields the MA coefficients $b[n]$, $n = 0, 1, \dots, Q$. The overall technique was observed to produce similar results as Durbin's method (see Section 4) at significantly reduced computational complexity.

Criteria for selecting the MA model order Q are discussed in [3]. We found that for good approximation accuracy, the MA filter should have the same length as the central (dominant) part of the subsampled autocorrelation $r'[n]$. For a Doppler bandwidth of 10^{-4} and subsampling factor $L = 1000$, we obtained good results with $Q = 100 \dots 1000$.

3. MULTISTAGE INTERPOLATOR

To compensate for the subsampling of $r[n]$ in (1), the output $h'[n]$ of the subsampled ARMA filter is interpolated by the subsampling factor L . If L is chosen as a composite number, i.e., $L = \prod_{k=0}^{K-1} L_k$, a particularly efficient *multi-stage* interpolator [5] can be used. Here, interpolation by L is performed by K successive interpolator stages with interpolation factors L_k . Each interpolator stage is represented using a polyphase decomposition. The input-output relations of the individual interpolator stages are [5]

$$h^{(k+1)}[n] = \sum_{i=0}^{L_k-1} u_i^{(k)} \left[\left\lfloor \frac{n}{L_k} \right\rfloor - i \right], \quad k = 0, 1, \dots, K-1$$

(where $\lfloor \xi \rfloor$ denotes the largest integer $\leq \xi$), with

$$u_i^{(k)}[n] = \sum_{l=-V_k}^{V_k-1} p_i^{(k)}[l] h^{(k)}[n-l], \quad i = 0, 1, \dots, L_k-1. \quad (9)$$

Here, $h^{(k)}[n]$ and $h^{(k+1)}[n]$ are the input and output, respectively, of the k th interpolator stage (in particular, $h^{(0)}[n] = h'[n]$ and $h^{(K)}[n] = h[n]$, cf. Fig. 1), and $p_i^{(k)}[n]$ and $u_i^{(k)}[n]$ are the impulse response (of length $2V_k$) and output sequence, respectively, of the i th polyphase filter of the k th interpolator stage.

We propose a mean square error (MSE) optimal design of the multistage interpolator that is analogous to the “deterministic MSE design” described in [5, Sec. 4.3.6]. The k th interpolator stage is designed such that the MSE

$$\text{MSE}^{(k)} \triangleq \text{E}\{|h^{(k+1)}[n] - \tilde{h}^{(k+1)}[n]\}^2$$

is minimized. Here, $\tilde{h}^{(k+1)}[n]$ is the output of an ideal low-pass interpolator with appropriate cutoff frequency.

The output signals of the polyphase branches within the k th interpolator stage are nonoverlapping in time and thus orthogonal. Hence, $\text{MSE}^{(k)} = \sum_{i=0}^{L_k-1} \text{MSE}_i^{(k)}$ with

$$\text{MSE}_i^{(k)} = \text{E}\{|u_i^{(k)}[n] - \tilde{u}_i^{(k)}[n]\}^2,$$

where $\tilde{u}_i^{(k)}[n] = \sum_{l=-\infty}^{\infty} \tilde{p}_i^{(k)}[l] h^{(k)}[n-l]$ (cf. (9)) is the output signal of an ideal interpolator polyphase filter with transfer function $\tilde{P}_i^{(k)}(\nu) = e^{j2\pi i\nu/L_k}$ [5]. This means that the individual polyphase filters $p_i^{(k)}[n]$ can be designed independently by separately minimizing the MSE components $\text{MSE}_i^{(k)}$. It is easily verified that $\text{MSE}_i^{(k)}$ can be expressed in the frequency domain as

$$\text{MSE}_i^{(k)} = \int_{-1/2}^{1/2} |P_i^{(k)}(\nu) - \tilde{P}_i^{(k)}(\nu)|^2 S^{(k)}(\nu) d\nu. \quad (10)$$

Here, $S^{(k)}(\nu) = \sum_{n=-\infty}^{\infty} r^{(k)}[n] e^{-j2\pi\nu n}$, with $r^{(k)}[n] = r[nI_k]$, $I_k = \prod_{i=k}^{K-1} L_i$, is the Doppler spectrum of the input process of the k th interpolator stage. Inserting $P_i^{(k)}(\nu) = \sum_{n=-V_k}^{V_k-1} p_i^{(k)}[n] e^{-j2\pi\nu n}$ and $\tilde{P}_i^{(k)}(\nu) = e^{j2\pi i\nu/L_k}$ into (10) and setting the derivatives of the resulting expression with respect to $p_i^{(k)*}[n]$ ($n = -V_k, \dots, V_k-1$) equal to zero [3], we obtain the following equations for the MSE-optimal interpolator coefficients $p_i^{(k)}[n]$,

$$\sum_{l=-V_k}^{V_k-1} p_i^{(k)}[l] r^{(k)}[n-l] = r^{(k+1)}[nL_k+i], \quad n = -V_k, \dots, V_k-1.$$

This can be written as

$$\mathbf{R}^{(k)} \mathbf{p}_i^{(k)} = \mathbf{r}_i^{(k+1)}, \quad (11)$$

with the vectors $\mathbf{p}_i^{(k)} = [p_i^{(k)}[-V_k] \dots p_i^{(k)}[V_k-1]]^T$, $\mathbf{r}_i^{(k+1)} = [r^{(k+1)}[-V_kL_k+i] \dots r^{(k+1)}[(V_k-1)L_k+i]]^T$ and the Hermitian Toeplitz matrix $\mathbf{R}^{(k)}$ with first row $[r^{(k)}[0] \dots r^{(k)}[-2V_k+1]]$. Since $\mathbf{R}^{(k)}$ does not depend on i , (11) is best solved by explicitly inverting $\mathbf{R}^{(k)}$ using the Levinson algorithm [3, 4], which has to be done only once per interpolator stage k .

The MSE-optimal multistage interpolator explicitly depends on the exact shape of the specified Doppler spectrum $S(\nu)$. If this dependence is undesired, one may employ a suboptimal default design using a rectangular $S(\nu)$ that is constant within the Doppler bandwidth and zero outside.

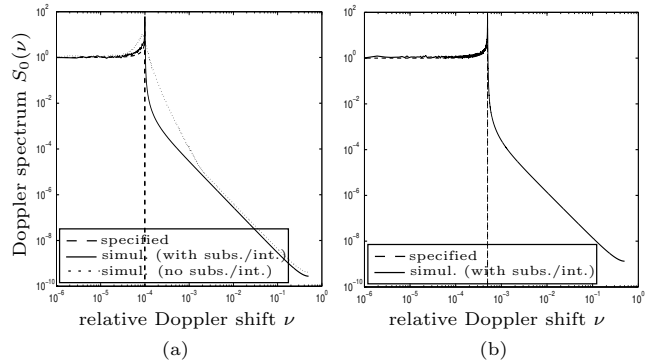


Figure 2: Simulation of a single-tap channel: (a) Specified (Jakes) Doppler spectrum, simulated Doppler spectrum, and simulated Doppler spectrum obtained without subsampling/interpolation; (b) simulated Doppler spectrum obtained at the output of the second interpolator stage.

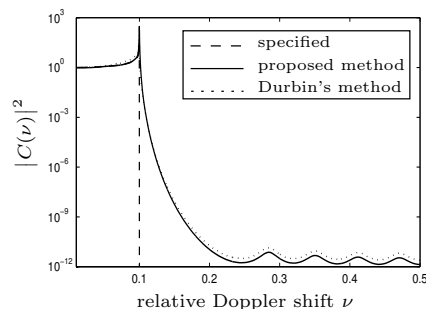


Figure 3: Squared magnitude of the frequency responses of the subsampled ARMA filter obtained with the proposed MA design method and with Durbin's method.

4. SIMULATION RESULTS

4.1. Simulation 1: Jakes Doppler Spectrum

Fig. 2 and Fig. 3 consider the simulation of a single-tap channel ($M = 1$) with a Jakes Doppler spectrum [1]

$$S_0(\nu) = \begin{cases} \frac{\nu_{\max}}{\sqrt{\nu_{\max}^2 - \nu^2}}, & |\nu| \leq \nu_{\max}, \\ 0, & \text{else.} \end{cases}$$

The relative Doppler bandwidth was $\nu_{\max} = 10^{-4}$ (corresponding, e.g., to an absolute Doppler bandwidth of 100 Hz when a sampling frequency of 1 MHz is used). The subsampling/interpolation factor was chosen as $L = 1000$. An ARMA filter of order $P = 20$, $Q = 100$ was designed using parameters $N = 200$ and $\gamma = 6 \cdot 10^{-10}$. The multistage interpolator comprised 3 stages with $L_0 = 5$, $L_1 = 40$, $L_2 = 5$ and polyphase filter lengths $V_0 = 5$, $V_1 = 2$, $V_2 = 10$. It was designed using a rectangular default Doppler spectrum.

Fig. 2(a) shows the specified (Jakes) Doppler spectrum $S_0(\nu)$ of the tap process $h_0[n]$ as well as an estimate of the Doppler spectrum of the simulated channel (estimated from 200 realizations of $h_0[n]$ with length 10^6 each.) It can be seen that the approximation is very accurate. Fig. 2(a) also shows the estimated Doppler spectrum obtained with an ARMA channel simulator that used the same ARMA model order ($P = 20$, $Q = 100$) but *no* subsampling/interpolation. It is seen that for a given ARMA model order, the sub-

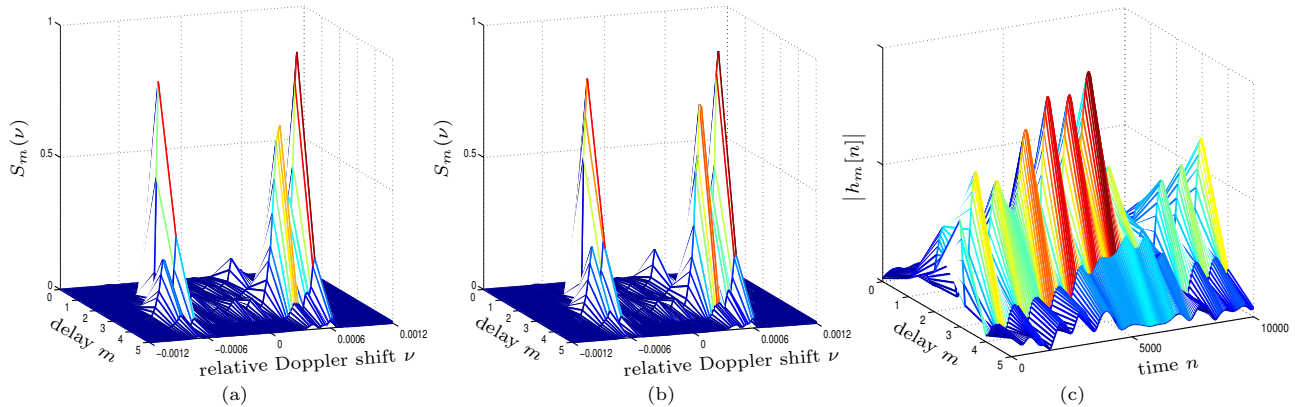


Figure 4: Simulation of a realistic channel: (a) Specified scattering function (estimated from measured channel data); (b) simulated scattering function (estimated from realizations of the simulated impulse response); (c) magnitude of a realization of the simulated impulse response.

sampling/interpolation technique yields a substantial performance improvement. (In fact, without subsampling/interpolation, an MA order of $Q = 10^4 \cdots 10^5$ would be needed to obtain a comparable performance.)

Fig. 2(b) shows an estimate of the Doppler spectrum of the simulated tap process at the output of the second interpolator stage (i.e., before the final interpolator stage). Since the interpolation factor of the final interpolator stage is $L_2 = 5$, the tap process after the second interpolator stage has Doppler bandwidth $L_2\nu_{\max} = 5 \cdot 10^{-4}$. This shows that it is possible to simultaneously generate channels with equal Doppler profile but different Doppler bandwidths.

Fig. 3 compares the frequency responses of the subsampled ARMA filter obtained with our MA design method (see Subsection 2.2) and with Durbin’s method [3, 4]. Identical AR coefficients were used. Note that these frequency responses do not include the interpolator; the Doppler bandwidth of 0.1 in Fig. 3 corresponds to a Doppler bandwidth of 10^{-4} after interpolation by $L = 1000$. It can be seen that our efficient method achieves slightly better stop-band attenuation than Durbin’s method.

4.2. Simulation 2: Realistic Channel

Fig. 4(a) shows a specified scattering function that was estimated [14] from channel data measured in a suburban area.¹ To each one of the $M = 6$ specified Doppler spectra $S_m(\nu)$, $m = 0, 1, \dots, 5$, we designed a corresponding subsampled ARMA filter of order $P = 50$ and $Q = 1000$ using parameters $N = 500$ and $\gamma = 10^{-5}$. The subsampling/interpolator parameters were as in Subsection 4.1. Fig. 4(b) shows an estimate of the scattering function $S_m(\nu)$ derived from 200 realizations of the simulated impulse response (tap processes) $h_m[n]$, $m = 0, 1, \dots, 5$, each of length $5 \cdot 10^5$. It is seen that the channel simulator achieves a good approximation of the specified scattering function. Finally, a segment of a simulated impulse response $h_m[n]$ is shown in Fig. 4(c).

5. CONCLUSIONS

We have presented a technique for simulating time-varying mobile radio channels that is specifically suited to the small

relative Doppler bandwidths encountered in wideband CDMA and OFDM communications. The combination of a “subsampled” ARMA innovations filter with a multistage interpolator was shown to yield substantial advantages regarding accuracy, efficiency, and flexibility.

REFERENCES

- [1] W. C. Jakes, *Microwave Mobile Communications*. New York: Wiley, 1974.
- [2] P. A. Bello, “Characterization of randomly time-variant linear channels,” *IEEE Trans. Comm. Syst.*, vol. 11, pp. 360–393, 1963.
- [3] C. W. Therrien, *Discrete Random Signals and Statistical Signal Processing*. Englewood Cliffs (NJ): Prentice Hall, 1992.
- [4] S. M. Kay, *Modern Spectral Estimation*. Englewood Cliffs (NJ): Prentice Hall, 1988.
- [5] R. E. Crochiere and L. R. Rabiner, *Multirate Digital Signal Processing*. Englewood Cliffs (NJ): Prentice Hall, 1983.
- [6] J. K. Cavers, *Mobile Channel Characteristics*. Boston (MA): Kluwer, 2000.
- [7] M. F. Pop and N. C. Beaulieu, “Limitations of sum-of-sinusoids fading channel simulators,” *IEEE Trans. Comm.*, vol. 49, no. 4, pp. 699–708, 2001.
- [8] P. Höher, “A statistical discrete-time model for the WSSUS multipath channel,” *IEEE Trans. Veh. Technol.*, vol. 41, no. 4, pp. 461–468, 1992.
- [9] G. Wetzker, U. Kaage, and F. Jondral, “A simulation method for Doppler spectra,” in *5th IEEE Int. Symposium on Spread Spectrum Techniques and Applications*, pp. 517–521, 1998.
- [10] G. B. Giannakis and C. Tepedelenlioglu, “Basis expansion models and diversity techniques for blind identification and equalization of time-varying channels,” *Proc. IEEE*, vol. 86, pp. 1969–1986, Oct. 1998.
- [11] D. H. Johnson and D. E. Dudgeon, *Array Signal Processing*. Englewood Cliffs (NJ): Prentice Hall, 1993.
- [12] J. Salz, “Optimum mean-square decision feedback equalization,” *Bell Syst. Tech. J.*, vol. 52, pp. 1341–71, Oct. 1973.
- [13] A. V. Oppenheim and R. W. Schaffer, *Digital Signal Processing*. Englewood Cliffs, NJ: Prentice Hall, 1975.
- [14] H. Artés, G. Matz, and F. Hlawatsch, “An unbiased scattering function estimator for fast time-varying channels,” in *Proc. 2nd IEEE Workshop on Signal Processing Advances in Wireless Communications*, (Annapolis, MD), pp. 411–414, May 1999.

¹Courtesy of T-Nova Deutsche Telekom Innovationsgesellschaft mbH, Technologiezentrum Darmstadt, Germany.